Article

Not peer-reviewed version

Albino Lethal 13, a Chloroplast Imported Protein Required for Chloroplast Development in Rice

Xiaoqiong Guo , Chunli Wang , Qian Zhu , Wenhua Dongchen , Xiaoling Zhang , Wei Li , Hui Zhang , Cui Zhang , Nant Nyein Zar Ni Naing , Mengting Li , Lijuan Chen * , Dongsun Lee *

Posted Date: 19 January 2024

doi: 10.20944/preprints202401.1472.v1

Keywords: albino leaf; OsAL13; RNA interference; chloroplast development; overexpression; rice (Oryza sativa L.)

Article

Albino Lethal 13, a Chloroplast Imported Protein Required for Chloroplast Development in Rice

Xiaoqiong Guo [1,6,†], Chunli Wang [1†], Qian Zhu [1,2,3], Wenhua Dongchen [4], Xiaoling Zhang [5], Wei Li [6], Hui Zhang [4], Cui Zhang [1], Nant Nyein Zar Ni Naing [1], Mengting Li [1], Lijuan Chen [1,2,3,*] and Dongsun Lee [1,2,3,*]

1 Rice Research Institute, Yunnan Agricultural University, Kunming 650201, China; 454282556@qq.com(X.G.); wchunli1989@163.com (C.L.);gbriel731@yuan.edu.cn(Q.Z.);1942669465@qq.com; (C.Z.); nyeinzarninaing@gmail.com (N.Z.N.N.); 991439160@qq.com (M.L.);
2 State Key Laboratory for Conservation and Utilization of Bio-Resources in Yunnan, Yunnan Agricultural University, Kunming 650201, China;
3 The Key Laboratory for Crop Production and Smart Agriculture of Yunnan Province, Yunnan Agricultural University, Kunming 650201, China;
4 College of Agronomy and Biotechnology, Yunnan Agricultural University, Kunming 650201, China; 627723479@qq.com (W.D.); 627637829@qq.com) (H.Z.)
5 Kunming University, Kunming 650214, China; 350340959@qq.com (X.Z.)
6 College of Biological Resource and Food Engineering, Qujing Normal University, Qujing 655011, China. muzikok@qq.com (W.L.)
* Correspondence: 454282556@qq.com (L.C.); dong_east@hanmail.net (D.L.)
† These authors contributed equally to this work.

Abstract: The chloroplast is important organelle responsible for photosynthesis and various bio-synthetic functions essential to green plants. However; the regulatory mechanism of chloroplast de-velopment remains elusive. Here, we characterized a mutant with defective chloroplasts in rice (*Oryza sativa* L.) named it albino and lethal 13(*osal13*), which exhibited a distinct albino phenotype in leaves, eventually leading to seedling lethality. Molecular cloning revealed that *OsAL13* encodes a novel protein in rice for which no homologous gene or known conserved domain was found. Analysis of the biological characteristics showed that the RNAi2 leaf was com-pletely albino phenotype, the root and shoot lengths were significantly inhibited compared with wild type. Transmission electron microscopy indicated that RNAi2 were defective in chloroplast development. Overexpression of *OsAL13* resulted the photosynthetic rate increase, So the total grain number per panicle also would be significantly increase. Besides, *OsAL13* was located in chloroplast and constitutively expressed in various tissues, including green and non-green tissues. In addition, disruption of *OsAL13* resulted in altered expression of plastid-encoded polymerases and nuclear-encoded chloroplast genes, *OsAL13* also affected hormone levels in plant tissues. Therfore, our results provide new insights into the role of *OsAL13* in regulating chloroplast development in rice

Keywords: albino leaf; *OsAL13*; RNA interference; chloroplast development; overexpression; rice (*Oryza sativa* L.)

1. Introduction

Chloroplasts are the main site of photosynthesis, which not only convert light energy into chemical energy, but also synthesize biologically essential compounds such as fatty acids, vitamins, amino acids, and tetrapyridine [1]. However defects of chloroplast development will affect leaf color, seeding survival or crop yield [2-3]. Therefore, the new rice leaf color mutants provide not only ideal materials for studying chloroplast development, but also important germplasm resources for high photosynthetic efficiency breeding in rice.

In general, chloroplasts develop from a proplastid to mature chloroplast is a complicated physiological process, which requires plastid DNA replication, build-up of chloroplast translation system, assembly of the photosynthetic apparatus and involves different regulatory genes [4]. So far,

 doi:10.20944/preprints202401.1472.v1

many of genes associated with albino phenotype in rice have been identified. The genes of *OsPPR1*, *ASL2*, *OsDjA7/8*, *AL1*, *OsPPR6*, *TCD5*, *OsCAF2*, *OsHMBPP*, *OsPPR9*, *ALS1*[5-14] were necessary for chloroplast development. Additionally, chloroplasts genes are transcribed by two distinct polymerases: nucleus-encoded polymerase (NEP) and plastid-encoded polymerase (PEP) [15]. Currently, at least 215 transcription start sites of PEP and NEP have been determined in mature chloroplasts of Arabidopsis using Terminome-seq [16].

Mutant of leaf color can be derived from a wide range of sources, including spontaneous, artificially induced, insertion, and gene silencing mutations [17-19]. Li et al. [20] classified typical leaf color mutant phenotypes include albino, green, light green, striped, white, yellow, green and yellow types. Yoo et al. [21] divided rice leaf phenotypes into types, including green leaf, albino, stripe, retarded green, zebra stripe, yellow, and variegated color. Li et al. [22] classified rice leaf color mutations into light green, yellow, albino, and reversible green albino. According to the characteristics of the generation and development of albinism, the albino phenotypes can be further divided into lethal albino, temperature-sensitive regreening albino, reproductive regreening albino, etc. When the leaf becomes colored, the levels of growth-promoting phytohormones, such as auxin, cytokinin and gibberellin are reduced [23]. Abnormal chloroplast development in cells also leads to abnormal cell division. In Arabidopsis Atcls8 mutants, inhibition of chloroplast DNA replication leads to abnormal growth: leaf albinism and curling and reduced root length [24].

In this study, a rice albino mutant *osal13* was screened from a T-DNA insertion mutant library, and its genetic characteristics were analyzed by genetic population construction. The data showed that the albino trait was controlled by a single recessive nuclear gene. The target gene and its promoter were cloned and its function was predicted using bioinformatics. The spatiotemporal expression pattern and genetic function of the target gene were studied by constructing four different expression vectors, and β-glucuronidase (GUS) staining and quantitative real-time PCR (qRT-PCR) were used to reveal the expression pattern of the target gene. The number and ultrastructure of chloroplasts in mutant and RNAi were analyzed using fluorescence microscopy and transmission electron microscopy (TEM). The hormone contents in wild-type (WT), *osal13* mutants, and transgenic plants were determined by enzyme-linked immunosorbent assay to explore the regulation effect of *OsAL13* on hormones. Multiple chloroplast-associated genes were investigated. Overall, this study improved our understanding of *OsAL13* protein and revealed the molecular mechanism of *OsAL13* action in rice chloroplast development.

2. Results

2.1. Phenotypic characteristics of osal13 mutants

The *osal13* mutants were a T-DNA insertion mutation derived from plasmid vector pCAMBIA3300 transferred into japonica cv LiyuB. Under light conditions, at 2 day after germination (DAG), the wild type (WT)and *osal13* mutants showed the same phenotype. however, they could be partially distinguished at 3 DAG. At 4 DAG, the first true leaf grew in the bud sheath, and WT and *osal13* mutants could be completely distinguished (Figure 1A). Although it exhibited a more severe albino phenotype during early leaf development, the severe albino phenotype of *osal13* mutants eventually resulted in a lethal phenotype when they reached the four-leaf stage (Figure 1B). Thus, we concluded that *OsAL13* is required for rice development.

With a view to verifying whether the *osal13* mutants were involved in chloroplast development, fresh sheath tissues were observed under bright field microscopy (Figure 1C,D), which revealed that cells of *osal13* mutants cotyledons had an apparent lower density of chloroplasts than WT cotyledons. This suggested decreased chlorophyll content of the *osal13* mutants, in line with the pale green pigmentation of *osal13* mutants compared with WT chloroplasts. Therefore, chlorophyll and carotenoid contents were measured in WT and *osal13*. As expected, levels of both chlorophylls and carotenoids were significantly lower in *osal13* mutants (Figure 1E), demonstrating that the albino phenotype was caused by abnormal chlorophyll metabolism.

Preprints (www.preprints.org) | NOT PEER-REVIEWED | Posted: 19 January 2024 doi:10.20944/preprints202401.1472.v1

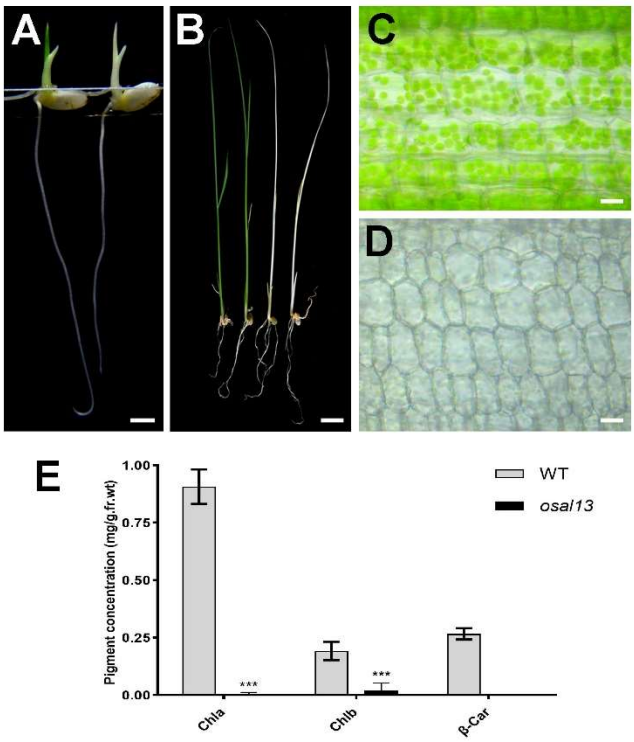

Figure 1. Mutations in the *OsAL13* gene affect the growth of rice and chloroplast development. (**A-B**): Phenotype analysis of the wild type (WT) and *osal13* mutants at 4 DAG and 20 DAG. Bars = 1 cm. (**C-D**): The sheath of wild type (WT) and *osal13* mutants visualized using bright-field microscopy. Scale is 25 μm. (**E**): Determination of pigment content in leaves of wild-type (WT) and *osal13* mutants. Leaf samples were collected from 20-day-old WT and *osal13* mutants grown in a tank containing nutrient solution. Chla, chlorophyll a; Chlb, chlorophyll b; and β-Car, β-carotenoid. Error bars are the standard deviation (SD) for three biological duplicates. Significant differences are indicated by asterisks ***$p < 0.001$.

2.2. Cloning of OsAL13

Genetic analysis indicated that the *osal13* mutants phenotype could be subject to control by a single recessive gene, as evidenced by the 3:1 segregation ratio between WT phenotypes and MT in the T_2 population (162 albino plants, 513 normal plants, $\chi^2 = 0.1961$). By DNA-walking technique, a specific amplified fragment including the fragment of CaMV3′UTR was obtained. The BLAST search with the flanking sequence indicated that the T-DNA was inserted into the OsJNBa0005p21 clone of rice chromosome 11 (Figure 2A,B and S1), which contained 21 predictive genes. The T-DNA was inserted into the third gene, Os11g0307600. A 662-bp specific fragment was obtained by amplification of specific primers *OsAL13*-1Fa and *OsAL13*-1Ra using LiyuB cDNA as a template. Sequencing results of the target band showed that there was a 453-bp ORF, which was identified as the target gene *OsAL13* (Figure 2D). The T-DNA was inserted before the base G of the start codon ATG (Figure 2C), causing the start codon to be misread and resulting in an albino phenotype. To investigate potential regulatory cis-acting elements, we analyzed the promoter region of *OsAL13* using PlantCARE-this detailed analysis revealed that it contained 19 different-regulatory elements involved in light responsive, hormone responsive, transcription, drought responsive (Table S1). Among of them, 9 regulatory cis-acting elements involved in light responsive. The *OsAL13* may have related light response functions.

Preprints (www.preprints.org) | NOT PEER-REVIEWED | Posted: 19 January 2024 doi:10.20944/preprints202401.1472.v1

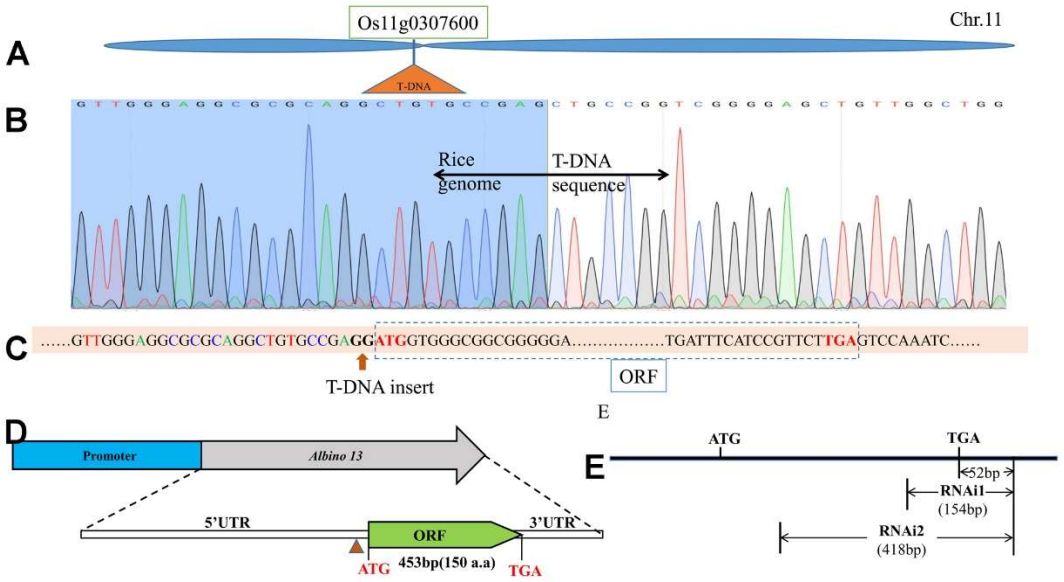

Figure 2. Positional cloning of the OsAL13 gene. T-DNA was inserted into Os11g0307600 at the short arm of chromosome 11 in rice. (**A**): The OsAL13 locus was narrowed to a 21-kb region on Os11g0307600. (**B**): The sequence peak chart of T-DNA insertion, the vertical division line indicates the point of T-DNA insertion. (**C**): T-DNA inserts before the base G of promoter ATG. (**D**): Structure of OsAL13, with ATG and TGA representing the start and stop codons, respectively. Blue boxes indicate the promoter and green boxes indicate the open reading frame (ORF). (**E**): Two different fragments for RNAi construction are shown as sketch maps.

2.3. Suppression of OsAL13 leads to osal13-like phenotype

The OsAL13 gene was seedling lethal, which caused difficulty in further study of the OsAL13 functions. To address this, we produced weak osal13 alleles by specific knockdown of OsAL13 expression. Two 154- and 418-bp WT genomic DNA fragments of Os11g0307600, containing part of the coding sequences, and part of the 3′UTR (52 bp) (Figure 2E), was cloned in a binary vector to generate the constructs of RNAi1 and RNAi2, and then transformed into WT (LiyuB). Finally, 22 independent RNA interference lines (RNAi1 and RNAi2) were obtained with different expression levels of OsAL13. Of these 22 independent RNAi lines, RNAi2-3, RNAi2-6, and RNAi2-8, with the most significant down-regulation of OsAL13, showed a highly similar phenotype to that of osal13 mutants (Figure 3A, B). The first and second leaves of WT, osal13 mutants, and RNAi2 plants were observed at the seedling stage. The first leaf of the WT was normal green, the osal13 mutants was completely albino, and of RNAi2 was yellow-green (Figure 3C). The second leaf of the WT was green, but the osal13 mutants and RNAi2 were white overall (Figure 3D). The shoot and root lengths of WT, osal13 mutants, and RNAi2 plants were measured. Root lengths of both osal13 mutation and RNAi2 plants were significantly inhibited compared with WT (Figure 3E). The albino osal13 mutants had significantly inhibited shoot length. Down-regulation of OsAL13 significantly inhibited root length and seedling growth (Figure 3F). These results further confirmed that OsAL13 was the candidate gene, was required for chloroplast development, and disruption of its function resulted in the albino leaf phenotype.

Preprints (www.preprints.org) | NOT PEER-REVIEWED | Posted: 19 January 2024 doi:10.20944/preprints202401.1472.v1

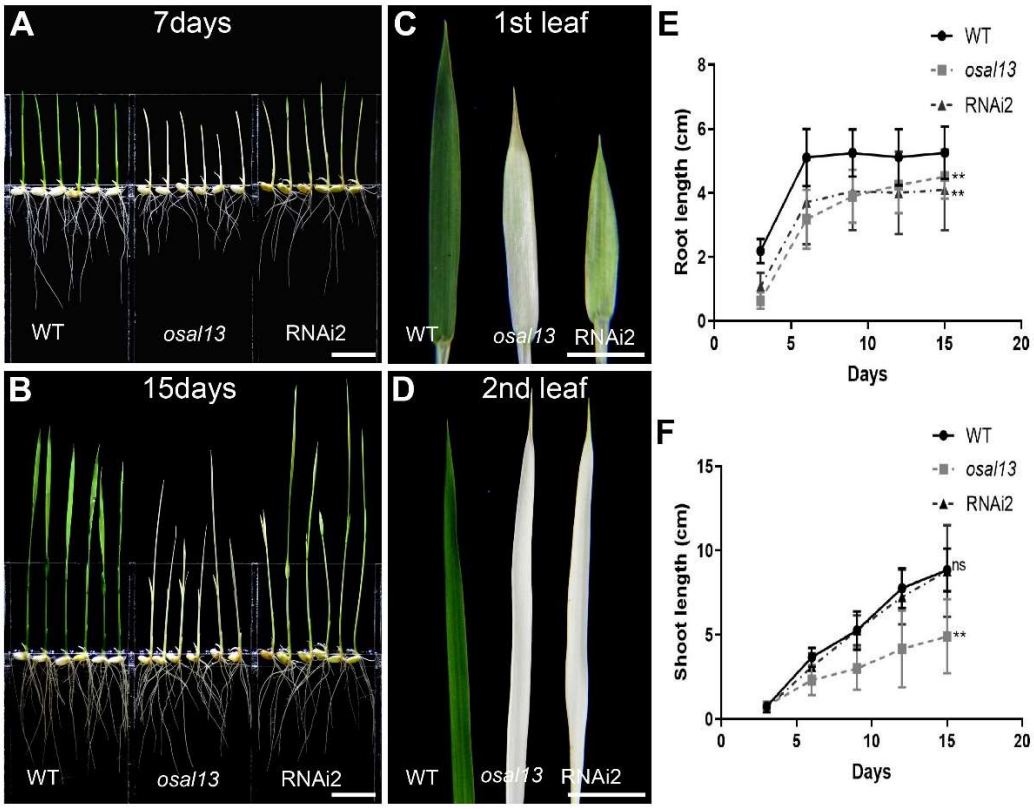

Figure 3. The different phenotypes of the wild-type, osal13 mutants and RNAi2. At 7 DAG (**A**) and 15 DAG (**B**). Bars = 1 cm. The comparison of the first (**C**) and second leaf (**D**) of the wild-type, osal13 mutants, and RNAi2. Bars = 1 cm. Seedling growth determination as root length (**E**) and shoot length (**F**), with data points representing the mean ± SD.

2.4. Subcellular localization and expression pattern of OsAL13

The OsAL13 protein was predicted to localize to chloroplasts using ChloroP 1.1 (http://www.cbs.dtu.dk/services/ChloroP/) (Emanuelsson et al., 1999) (Table S2). To investigate the subcellular localization of OsAL13 protein, the protoplasts of transgenic plants p35S::EGFP and p35S::OsAL13:EGFP were extracted. The green fluorescence signal was apparent over the whole cell in the EGFP positive control (Figure 4A-a-d and Figure S2). In p35S::OsAL13:EGFP, the green fluorescence signal co-localized with chloroplast autofluorescence (Figure 4A-e-h), suggesting that the target gene was expressed in the chloroplast. This result supported the view that *OsAL13* plays an important role in regulating chloroplast development. Different tissues from different growth stages of LiyuB were assayed for temporal and spatial expression patterns of *OsAL13* using qRT-PCR (Figure 4B). Transcripts of *OsAL13* were detected in all examined tissues and were most abundant in the leaves blade, and weakest in stem (Figure 4B).

We next examined the expression of the GUS gene under the control of the OsAL13 promoter from LiyuB in transgenic plants. All tissues exhibited GUS activity and the GUS signal was particularly strong in the root tip (Figure 4C, D) and shoot apical meristem (Fig. 4E). During leaf development, reporter genes were mainly expressed in young leaves (Fig. 4F). The GUS gene was expressed in the coleoptile and the first leaf of the bud sheath, and strongly expressed in the vascular sheath (Figure 4G, H). The GUS staining of the root tip at 4 DAG was performed by frozen section, and the target gene was mainly expressed in root epidermis, exodermis, sclerenchyma cells (Figure 4I) and in the meristem and growth region (Figure 4J). Longitudinal sectioning of the bud sheath showed that the target gene was mainly expressed in the meristem region, and undeveloped leaves; the target gene was expressed in all cells, especially leaf sheath cells. Our results suggested that *OsAL13* is constitutively expressed in a variety of tissues and primarily plays a role in green tissues and in places where cell growth is active.

Preprints (www.preprints.org) | NOT PEER-REVIEWED | Posted: 19 January 2024 doi:10.20944/preprints202401.1472.v1

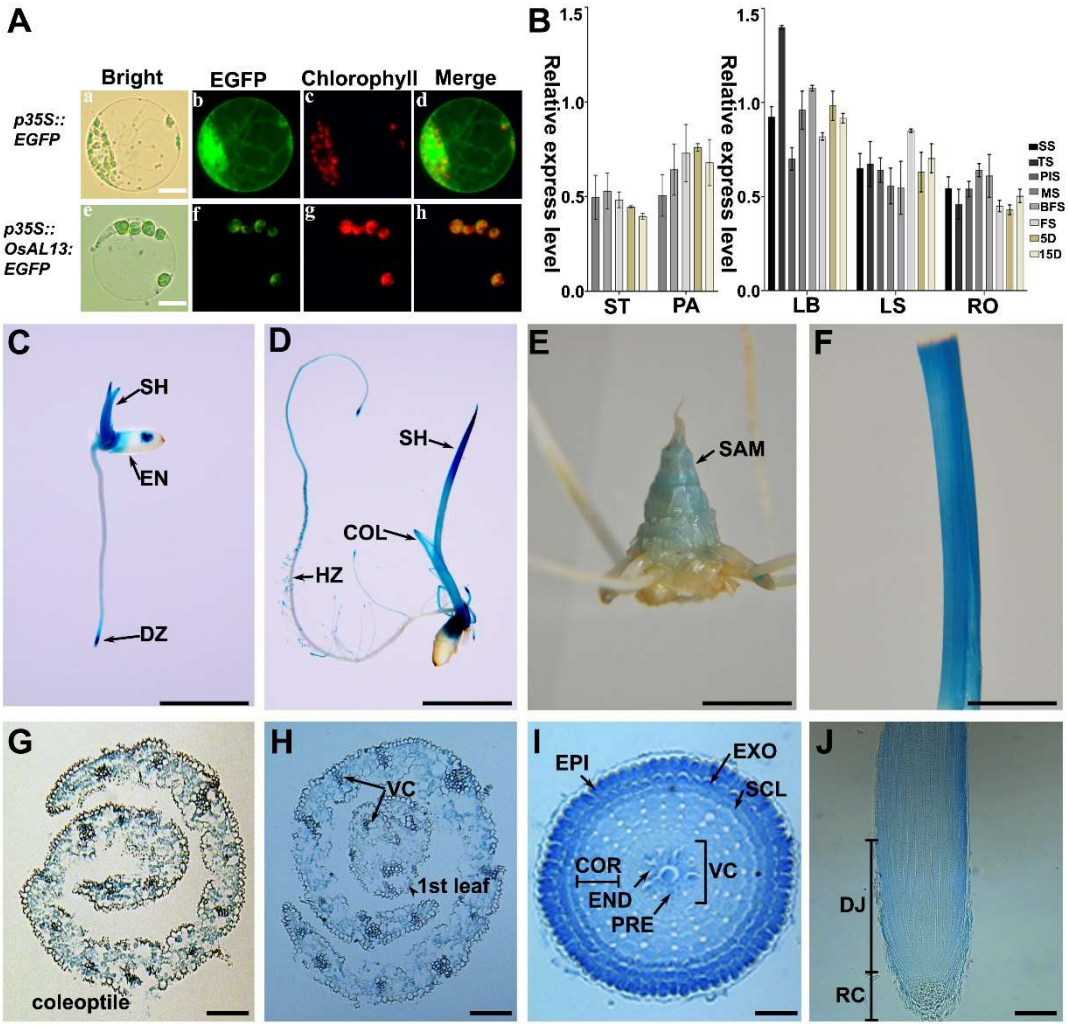

Figure 4. Subcellular location and expression pattern of *OsAL13*. (A): Analysis of the subcellular localization of the OsAL13 protein in rice protoplasts. Green fluorescence shows GFP. Chloroplast autofluorescence is shown in red. Scale bars are 50 μm. (B): qRT-PCR analysis of *OsAL13* in comparison with the rice β-actin gene. *OsAL13* expression was detected in the panicle (PA), stem (ST), leaf blade (LB), leaf sheath (LS) and root (RT) of the rice plant in seedling stage (SS), tiller stage (TS), panicle initiation stage (PIS), meiotic division phase of the rice panicle (flower) development (MS), before the flowering stage (BFS), flowering stage (FS), 5 days after pollination (5 D), and 15 days after pollination (15 D) of the rice plant. (C): GUS staining of seeds at 2 DAG. (D): GUS staining of seeds at 5 DAG. Histochemical staining showing *OsAL13* expression in the cell division zone (DZ), endosperm (EN), shoot (SH), root hair zone (HZ), and coleoptile (COL). (E): GUS staining of stem tip at the tillering stage; SAM, shoot apical meristem. (F): GUS staining of the leaf at meiotic phase of flag leaf. (G-H): GUS staining of the cross-sections from 5 DAG in the leaf primordia, as well as root tip (I) and (J). Abbreviations: VC, vascular cylinder; EPI, epidermis; EXO, exodermis; SCL, sclerenchyma; COR, cortex; END, endodermis; and PER, pericycle.

2.5. OsAL13 regulates related development of the photosynthetic system

The qRT-PCR analysis of WT, OVE, RNAi1, and RNAi2 plants indicated that transcript levels of *OsAL13* were increased in OVE and partially eliminated in the RNAi1 and RNAi2 (Figure 5A).

We further determined photosynthetic rates in WT, OVE, and RNAi plants, The RNAi lines showed significantly lower photosynthetic rates, but the OVE plants showed significantly higher photosynthetic rates plants compare to WT plants (Figure 5B). Because the mutants exhibited an albino phenotype, we speculate that the target gene might affect chlorophyll development. Therefore, disrupting expression of the target gene might lead to abnormal chloroplast. The chlorophyll content

Preprints (www.preprints.org) | NOT PEER-REVIEWED | Posted: 19 January 2024 doi:10.20944/preprints202401.1472.v1

was very much higher in WT than in RNAi1 and RNAi2 plants, and carotenoids were almost undetectable in RNAi lines (Figure 5C). We infer that inhibition of *OsAL13* expression affects the development of chlorophyll and carotenoids.

To further explore the regulation function of *OsAL13* in chloroplast development, we compared the chloroplast ultrastructure of RNAi and WT plants. As expected, WT cells contained normal chloroplasts, had good lamellar structure, normal stacked grana and thylakoids. In contrast, most RNAi cells had predominantly undeveloped chloroplasts and these were small. They also lacked thylakoids with grouped or layered structure, and some chloroplasts showed internal vacuolation (Figure 5D).

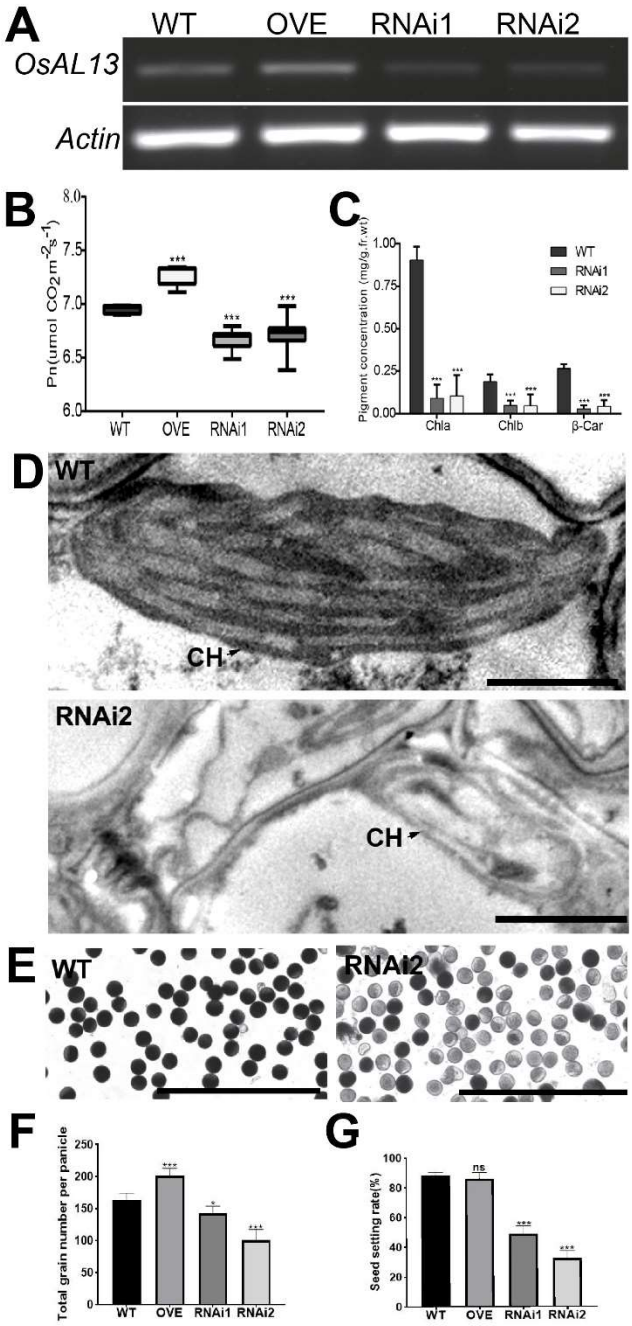

Figure 5. Comparison of the morphology and internal structure of WT, OVE, and RNAi lines. (**A**): Expression analysis of *OsAL13* in seedings at 7 DAG of the WT, *OsAL13* overexpressing (OVE), RNAi1, and RNAi2 lines by qRT-PCR. (**B**): Photosynthetic rate of WT, OVE, RNAi1, and RNAi2. (**C**): Determination of pigment contents in leaves of WT, RNAi1, and RNAi2. Leaf samples were collected from 20-day-old WT, RNAi1, and RNAi2 plants grown in a tank containing nutrient solution. Chla,

 doi:10.20944/preprints202401.1472.v1

chlorophyll a; Chlb, chlorophyll b; Car, carotenoid. Transmission electron microscopy observations of the third-leaf sections of WT and RNAi2. The ultrastructure of chloroplasts of WT is typical. The chloroplast structure is complete, the matrix is dense, and the grana lamellae are arranged along the long axis of the chloroplast. (**D**): The thylakoid structure of WT is clear, whereas the shape of chloroplast of the RNAi2 became irregular and the whole chloroplast shows a vesicle structure. Scale bars are 10 μm. (**E**): Pollen viability assay by I2-KI in WT and RNAi2 lines. Scale bars are 200 μm. Analysis of total grain number per panicle (**G**) and seed setting rate(**H**) of WT, OVE, and RNAi lines. Significant differences are indicated by asterisks ***$p < 0.001$.

2.6. Suppression of OsAL13 expression results in decreased pollen fertility and seed setting rate

Pollen fertility of WT was 94 ± 2.3% and of RNAi2 was 14 ± 3.4% (Figure 5E), the pollen fertility of RNAi2 plants were significantly reduced. And then, the total grain number per panicle of OVE plants were significantly increased, but the RNAi plants were significantly reduced (Figure 5F). The seed setting rate of RNAi plants were also significantly reduced (Figure 5G). So the total grain number per panicle and seed setting rate of RNAi2 was significantly lower. The other yield-related agronomic traits of WT and transgenic RNAi plants were measured (Table 2). After *OsAL13* expression was inhibited, plant height was reduced with less effect on effective panicle number, panicle length, number of primary branches, number of secondary branches, and grain length, but the effects on grain length, and grain thickness were greater. Combined with the previous pollen fertility, we speculated that the decrease in pollen fertility could lead to a decrease in seed setting rate.

Table 2. Analysis of yield-related characters (per plant) among wild-type and OsAL13-RNAi plants.

Traits	Wild-type	AL13-RNAi1	AL13-RNAi2
Plant height (cm)	87.40 ± 3.10	80.20 ± 1.70*	68.50 ± 3.50***
Tillering numbers	4.40 ± 1.10	4.60 ± 1.50	5.80 ± 1.80
Panicle length (cm)	20.10 ± 1.60	16.10 ± 1.60***	18.80 ± 2.00
No. of primary branches	10.00 ± 2.30	8.90 ± 2.30	9.90 ± 1.50
No. of secondary branches	21.20 ± 6.50	13.10 ± 7.00	20.40 ± 5.70
Grain length (mm)	7.03 ± 0.25	7.09 ± 0.09	7.00 ± 0.07
Grain width (mm)	3.16 ± 0.15	2.97 ± 0.13***	2.96 ± 0.11***
Grain thickness (mm)	2.25 ± 0.07	2.11 ± 0.07***	2.07 ± 0.07***

2.7. OsAL13 affects hormone levels in plant tissues and alters expression of chloroplast-associated genes

The endogenous hormones indoleacetic acid (IAA), gibberellin A3(GA3), and Cytokinin (CTK)were measured in the shoots and roots of WT, *osal13* mutants (MT), OVE, and RNAi plants (Figure 6). In the shoots, the CTK contents of RNAi2 was significantly increase, the IAA contents of MT, RNAi line were significantly higher than WT, but the IAA contents of OVE were significantly lower than WT. However, the GA3 contents have opposite trend with IAA in the shoots of MT, RNAi,

Preprints (www.preprints.org) | NOT PEER-REVIEWED | Posted: 19 January 2024 doi:10.20944/preprints202401.1472.v1

and OVE (Figure 6A,C,E). The contents of CTK in the shoots of OVE were significantly decreased, while in the shoots of RNAi2 were significantly increased compared with WT. CTK contents in the roots of MT and RNAi were higher than WT, while there were as no significant differences in CTK contents between OVE and WT. The contents of IAA in the root of OVE have higher levels, while the MT roots were not significant differences, the RNAi roots have lower levels compared with WT. The contents of GA3 in the roots of MT, OVE, RNAi were not significant difference compared with WT (Figure 6B, D,F). Thus, *OsAL13* overexpression led to enhanced IAA level in the roots and increased GA3 level in the shoot.

In higher plants, chloroplast genes are transcribed by two types of RNA polymerases: nucleus-encoded polymerases (NEP) and plastid-encoded polymerases (PEP). To confirm the role of *OsAL13* in the biological process of chloroplast development, multiple chloroplast-associated genes were analysis by qRT-PCR. In the WT, the expression levels of three PEP genes (psaA, psaB, and rps14) were down-regulated whereas that of the other (psbA) was up-regulated (Figure 6G). Nevertheless, the transcript levels of the two nuclear-encoded chloroplast genes (petA and rps2) were significantly impaired in the WT, whereas expression of atpA was up-regulated and rpoB was not significantly changed (Figure 6H). These results indicate that the chloroplast expression system that utilizes PEP and NEP was deficient in the WT and led to defective chloroplast biogenesis.

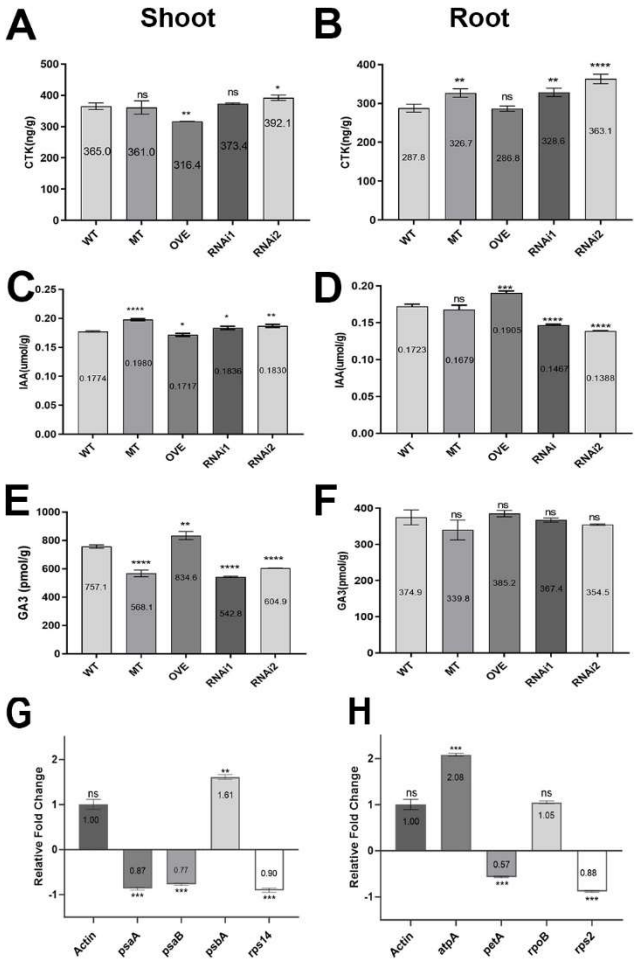

Figure 6. *OsAL13* control of hormone distribution and expression of chloroplast-associated genes. Hormone content comparison among WT, *osal13* mutants, OVE, and *OsAL13*-RNAi plants at seedling stage. Contents of CTK, IAA, and GA3 in shoot (A, C, E) and root (B, D, F). Values are mean ± SD. Asterisks indicate significant differences: *$p < 0.05$, **$p < 0.01$, and ***$p < 0.001$. The relative fold change of the chloroplast-associated genes including plastid-encoded polymerases (G) and nucleus-encoded polymerases (H) by qRT-PCR.

3. Discussion

 doi:10.20944/preprints202401.1472.v1

Using a DNA-walking cloning method, we isolated the gene *OsAL13*, which encodes a novel protein. We found that *OsAL13* is a novel gene in rice that has not been cloned or studied. The protein sequence encoded by *OsAL13* is shown in (Figure S3). Searching for the conserved domain of the protein encoded by *OsAL13* in the NCBI was not successful (Figure S4). Homologous genes and homologous proteins were found, but no homologous proteins (genes) with known functions were found (Figure S5).

In the *OsAL13* mutations, the most obvious phenotypic feature was albino lethality. In previous studies, the gene that caused the albino lethality phenotype basically affected chloroplast development and chlorophyll metabolism abnormality [25-27]. The rice albinism seedling mutants *Oslas1*, *Osasl4*[28], *Osra1* [29] and *OsCpn60β1* [30] also showed albino phenotype and eventually died, and chlorophyll contents were significantly reduced. Similarly, chlorophyll a and chlorophyll b of *osal13* mutants were significantly lower than those of WT. The RNAi tests verified that *OsAL13* was responsible for the albino phenotype (Figure 3A, B). Hence *OsAL13* is essential for chloroplast development.

Our results suggest that *OsAL13* was constitutively expressed and had a high level of transcription in leaves, suggesting that *OsAL13* may play an important role in leaf development. Subcellular localization in rice protoplasts showed that OsAL13 protein was located in chloroplasts (Figure 4A). Further research showed that the pigment concentration of RNAi plants was decreased significantly (Figure 5B,C) and the chloroplast structure was not complete, especially there was a lack of neatly stowed thylakoid structure (Figure 5E). The thylakoid is important for the synthesis of photosynthetic pigment and fixation of light energy by photosynthesis. Functional chloroplasts are the main sites of photosynthesis, providing both a relatively independent space environment and key proteins for their successful operation, thus establishing the photosynthetic autotrophic conditions of plants [31]. Meanwhile the photosynthetic rate of OVE plant was highest, so the total grain number per panicle of OVE plant would be significantly increase. Therefore, *OsAL13* is a necessary gene for chloroplast development.

It is well known that a chloroplast develops from a simple and undeveloped proplastid during light-dependent differentiation [32]. The chloroplast is a semi-autonomous organelle containing about 100 genes, although more than 3000 proteins function within it [33]. Thus, nuclear-encoded factors play essential roles in regulating chloroplast development, which requires the coordinated expression of both nucleus and chloroplast-encoded genes. The *osal13* mutants disrupts the transcripts of plastid and nuclear genes associated with chloroplast development (Figure 6). The transcript accumulation of both PEP- and NEP-dependent genes (*PetA* and *rps2*) and PEP-transcribed plastid genes (*psaA* and *psaB*) was severely suppressed (Figure 6G and H), suggesting that accumulation of transcripts for PEP components did not result in the formation of functional PEP due to the disruption of transcription/translation apparatus.

Carotenoids are a class of isoprene compounds synthesized in collaboration with chlorophyll and play many important roles in all photosynthetic organisms [34]. For example, in addition to stabilizing membranes (including thylakoid membranes) and promoting photomorphogenesis, many carotenoid molecules also act as auxiliary pigments, assisting chlorophyll to capture light energy and transfer it to the photosystem, from which excess energy can be transferred, reducing oxidative stress in the photosystem [35]. Therefore, lack of carotenoid protection during chloroplast development may cause metabolic disorders, such as accumulation of reactive oxygen species and abnormal energy metabolism. In this paper, carotenoids were nearly undetectable in *Osal13*, and whether this will lead to plant metabolic disorders, accumulation of reactive oxygen species, and abnormal energy metabolism requires further exploration.

In this study, expression of endogenous hormones showed that, compared with WT, GA3 content significantly rose in shoots of OVE plants, but significantly declined for *osal13* mutants and RNAi shoots. Previous studies indicated that GA3 in Arabidopsis promote chloroplast cell division and cell expansion of chloroplast [36]. The CTK has a positive effect on chloroplast development. In Arabidopsis, bud removal activates CTK signaling mediated by Arabidopsis respons39e modulator B, induces chlorophyll accumulation and photosynthetic remodeling, and promotes chloroplast

Preprints (www.preprints.org) | NOT PEER-REVIEWED | Posted: 19 January 2024 doi:10.20944/preprints202401.1472.v1

formation in isolated root cells [37]. In rice, GA3 controls cell division by stimulating the expression of some cyclins and CDK genes to activate G1/S and G2/M transitions [38]. Therefore, we speculate that *OsAL13* may regulate chloroplast proliferation through endogenous plant hormones.

In summary, O*sAL13* was essential for chloroplast development. Additionally, *OsAL13* had preferentially expressed in leaves blade and was localized in the chloroplast, and involved in rice hormone regulation. Disruption of *OsAL13* resulted in altered expression of plastid-encoded polymerases and nuclear-encoded essential genes for chloroplast development. Consequently. the *OsAL13* clearly functioned in the molecular mechanism of chloroplast development, and this lays a foundation for further excavation and utilization of chloroplast development genes and albino mutants in hybrid breeding and high light efficiency breeding.

4. Materials and Methods

4.1. Plant materials and growth conditions

The O. sativa japonica cv LiyuB was used as the WT. The T-DNA insertion library with LiyuB background was obtained from the Rice Research Institute of Yunnan Agricultural University. Because the albino mutants die at the four-leaf seedling stage, individual plants were harvested to preserve seeds of the heterozygote. All rice seeds were propagated under natural growing conditions in a tightly controlled greenhouse at the Rice Research Institute of Yunnan Agricultural University (Kunming, China).

4.2. Analysis of the T-DNA insertion locus in osal13 mutant

Genomic DNA of *osal13* albino mutant (MT) was extracted by the CTAB method at 1 week after germination. DNA-walking was performed using DNA Walking Speedup TM Premix Kit (http://www.seegene.com). The target region was obtained by the first round of PCR amplification with the highly specific renaturation control primers (DW-ACP2) and the target specific primers (Bar_TSP1). The first round of PCR products was used as the template, and the second round of amplification was carried out by the DW-ACPN and the target specific primer (Bar_TSP2) to narrow the target area. Finally, the second round of PCR products was used as the template, and the third round of amplification was carried out by the universal primer (Unip2) and the new target specific primer (Bar_TSP3) to obtain the different fragments. Primers for testing of the T-DNA inserting locus were Unip2 for the left site and Bar_TSP3 for the right. Primers sequences are listed in Table 1.

Table 1. List of primer sequences used in in this study.

Primer name	Primer Sequence (5′-3′)	Tm	Primer function
Bar_TSP1	ATGCACGAGGCGCTCGGATA		
Bar_TSP2	TCAAGCACGGGAACTGGCAT		
DW3ACP1	GAGGAGTGGCAGTGGGAACGGG	60℃	
DW3ACP2	GAGGAGTGGCAGTGGGCTCGA	60℃	
DW3ACP3	GAGGAGTGGCAGTGGGCTACG	60℃	Test al13 flanking of T-DNA
DW3ACP4	GAGGAGTGGCAGTGGGAACGG	60℃	
T-DNA right border	TGTTTACACCACAATATATCCTGCCA		
T-DNA left border	TGGCAGGATATATTGTGGTGTAAACA		
UniP2	GAGTTTAGGTCCAGCGTCCGT		
Bar_TSP3	TGCCCGTCACCGAGATCTGA		
OsAL13p-F	GAATTCGGATTCGTCCGTTGCCATGA	61℃	Promoter cloning

Preprints (www.preprints.org) | NOT PEER-REVIEWED | Posted: 19 January 2024 doi:10.20944/preprints202401.1472.v1

OsAL13p-R	CTGCAGGAGGCCAAGGTGGAGTTGG		
OsAL13-1Fa	CTGCAGGACGGCCAAGGCGTGCAG	64℃	*OsAL13* full length ORF amplification
OsAL13-1Ra	ACGCGTAGGGCGGATACCAAGTTCAACACGA		
OsAL13Ri-1F	CATCCCCCGAAATCAGGTTGG	57℃	RNAi1 short fragment amplification
OsAL13Ri-1R	GGGCGGATACCAAGTTCAACAC		
OsAL13Ri-2F	ATCCGGCGTCTTAGTTCTAGCC	58℃	RNAi2 short fragment amplification
OsAL13Ri-2R	GTGTTGAGGGAGCCAGGAAATC		
OsAL13RT-F	CTCATGGTTTGTCGCCTTCGTC	58℃	qRT-PCR
OsAL13RT-R	GGCGGATACCAAGTTCAACACG		
HmMAS-F	AGACCTGCCTGAAACCGAACTG	60℃	Transgenic plant screening
HmMAS-R	TGTTGGCGACCTCGTATTGGGA		
β-Actin-F	CCGAGCGGGAAATTGTGAGGGA	62℃	qRT-PCR housekeeping gene
β-Actin-R	TTTCAGGAGGGGCGACCACCTT		
psaA-F	TTAGAAATCCGCCAATCCA	53℃	
psaA-R	TGCTAGGCTCTACAACCATT		
psaB-F	GAGCAATATCGGTCAGCCACA	56℃	qRT-PCR Plastid-encoded polymerases (PEPs)
psaB-R	ACCACTCAAGGAGCGGGAAC		
psbA-F	ACCCTCATTAGCAGATTCGT	57℃	
psbA-R	GATTGTATTCCAGGCAGAGC		
rps14-F	TCACTCAAACTCAAAGGGTA	53℃	
rps14-R	AAGCGGCAGAAATTAGAAC		
atpA-F	TATCGGTCAAAGAGCATC	58℃	
atpA-R	CGTATAAGGAGCGAGGTA		
petA-F	TGCCATTTAGCGAATAAGCC	57℃	qRT-PCR Nucleus-encoded polymerases (NEPs)
petA-R	CCACATTCAACCCTCCCTTT		
rpoB-F	TGGTACATATCCCTTATCTCAA	53℃	
rpoB-R	CTCCAGGACCCAAACAACTC		
rps2-F	GAGATGATAGAAGCGGGAGTT	55℃	
rps2-R	TAACATAATGACAACGAGCC		

4.3. Gene cloning, characterization, and bioinformatic analysis

Sequence alignment analysis showed that the T-DNA was inserted into the Os11g0307600 gene. Two different transcripts, Os11t0307600-01 and Os11t0307600-02 encoding 128 and 522 amino acids, respectively, were found at this gene site by RAP-BD database retrieval. Primer5 software was used to design primers *OsAL13*-1F/-1Ra and OsAL13-1F/-2Rb on both sides of the predicted gene region, and PCR amplification was performed using LiyuB cDNA as the template.

The *OsAL13* gene was annotated according to the full-length cDNA sequence on the National Center for Biotechnology Information (NCBI) database. Sequence similarity was determined using the BLAST program (http://www.ncbi.nlm.nih. Gov/

BLAST/) provided by the NCBI website. Protein conserved domain analysis was performed using CD databases(https://www.ncbi.nlm.nih.gov/Structure/cdd/wrpsb.cgi).

4.4. Vector construction and transformation

Preprints (www.preprints.org) | NOT PEER-REVIEWED | Posted: 19 January 2024 doi:10.20944/preprints202401.1472.v1

The corresponding primers (Table 1) were amplified with the genomic DNA of LiyuB as the template to obtain the 2.3-kb DNA fragment of the promoter region of *OsAL13*, which was confirmed by DNA sequencing and then ligated into the binary vector HPE193-2. In order to obtain the over-expressing (OVE) plants, the corresponding primers were used to amplify a 610-bp DNA fragment including the full open reading frame (ORF) of *OsAL13* with LiyuB cDNA as the template, which was confirmed by DNA sequencing and then ligated into the binary vector HPE192-1. To construct the *OsAL13* RNAi vector (*p35S×2::OsAL13-RNAi*), a 117-bp intron fragment was used as a linker between a 154-bp gene specific fragment (a 418-bp gene specific fragment was generated synchronously) in the antisense and sense orientations. These recombined fragments were inserted into the HPE203-1 binary vector containing a double 35S promoter.

The final constructs were transferred into Agrobacterium tumefaciens strain EHA105 using the freeze-thaw method for rice genetic transformation. The rice transformations were conducted as described by Toki et al.,[39]. Eight OVE plants (*p35S::OsAL13:EGFP*), 12 GUS stained plants (*pAL13::GUS*), 11 RNAi1 plants (*p35S×2::OsAL13:RNAi1*), and 11 RNAi2 plants (*p35S×2::OsAL13:RNAi2*) were obtained in the T_0 generation.

4.5. Histological GUS assay

The GUS activity analysis was performed following a standard protocol (Jefferson et al., 1987). Tissues of rice at different periods were taken, cut into appropriate sizes, and immediately immersed in 90% acetone at -20°C for 15-20 min. Acetone was removed and the sample rinsed with rinse solution: 0.1 M $K_3Fe(CN)_6$, 0.1 M $K_4Fe(CN)_6$, and 0.5 M $NAPO_4$ at pH 7.2. The rinse solution was removed and X-GluC staining solution (10% Triton X-100, 20 mM X-GluC, 0.1 M $K_3Fe(CN)_6$, 0.1 M $K_4Fe(CN)_6$, and 0.5 M $NAPO_4$ at pH 7.2) was added in a test tube to ensure that the sample was completely immersed in the dye solution. At room temperature, the sample was vacuumed for 10-20 min to sink below the liquid level. The samples were treated overnight at 37℃. The samples were rinsed with 70% ethanol to remove the chlorophyll in leaves. The cleaned samples were observed under an anatomical lens and stained samples were photographed using a Nikon digital camera and further sliced using frozen sections (Leica CM1950, Leica Biosystems Nussloch GmbH, Nussloch, Germany) and analyzed under a dissecting microscope.

4.6. Total RNA extraction and qRT-PCR Analysis of Gene Expression

To explore the *OsAL13* expression pattern and level, total RNA was extracted from plant tissues at different developmental stages using a RNeasy Plant Mini Kit 50T (Cat. No. 74904; Qiagen; Germany) according to the manufacturer's instructions. The concentration of RNA samples was estimated using a spectrophotometer (NanoDrop 1000; Thermo Scientific Inc., Massachusetts, USA), and the quality of the RNA samples was examined using a 1.2% denatured agarose gel (Cat. No.111860; XHLY Co. Ltd., Beijing, China). The first strand of cDNA was synthesized using FastKing RT Kit (Cat. No. FP205-02; Tiangen Co.Ltd., Beijing, China) according to the manufacturer's protocol for qRT-PCR. All primers were designed using Primer 5 software (Table 1). The *β-actin* gene was used as an internal control. qRT-PCR was performed using a CFX96 Real Time System (Bio-Rad, Hercules Co. Ltd., New York, USA) and Super Real Premix Plus (SYBR Green) (Cat. No. FP205-01; Tiangen Co., Ltd., Beijing, China) according to the instructions. The relative quantification values were calculated using the $2^{-\Delta\Delta Ct}$ method [40], and three independent biological replicates were analyzed.

4.7. Confocal Microscopy

To identify the subcellular localization of *OsAL13*, the ORF of the target gene and the 610-bp fragment in the 5′UTR region of the target gene were successfully transferred into the EGFP vector HPE192-1 (preserved in our laboratory), and the corresponding transgenic plants were obtained by Agrobacterium-mediated genetic transformation method into the embryogenic callus of rice LiyuB. The protoplasts of the transgenic *p35S::OsAL13: EGFP* and *p35S: EGFP* were extracted as described by Poddar in previous studies[41].

 doi:10.20944/preprints202401.1472.v1

4.8. Endogenous hormone assay

In order to clarify whether *OsAL13* gene is involved in endogenous hormone regulation for plant. So we measured the auxin (IAA), gibberellin (GA3), and cytokinin (CTK) contents of the WT, *osal13* mutants (MT), OVE, RNAi1, and RNAi2 plants at 10 days after germination (DAG). Endogenous contents of IAA, GA3, and CTK were determined as described in previous studies [42].

4.9. Chlorophyll detection

During the seedling stage, fresh leaves were collected and sliced into small pieces. Of these, about 0.05 g was placed in a 15-mL tube, and 10 mL of 80% acetone was added. These were mixed in darkness for about 48 h (chlorophyll degrades under light). The extract was transferred to a 25-mL volumetric flask, diluted with 80% acetone to volume, and thoroughly mixed. Then, chlorophyll content was determined using absorbance (A: 663, 646, and 470 nm). The chlorophyll concentrations were calculated as follows (use 80% acetone as a blank control):

Chla (mg/g) = [12.21 × A663 - 2.81 × A646] × V/ (1000 × W),
Chlb (mg/g) = [20.13 × A646 - 5.03 × A663] × V/ (1000 × W),
Chla+b (mg/g) = [7.18 × A663 +17.32 × A646] × V/ (1000 × W),
β-Car (mg/g) = [(1000 × A470 - 3.27 × Chla -104 × Chlb)/229] × V/ (1000 × W),
where V is volume of extract (mL) and W is weight of fresh leaves (g).

4.10. Phenotype characterization

To explore the effect of target genes on the biological characteristics of rice, we measured the plant height, effective tiller, panicle length, seed setting rate, and primary and secondary branches of the WT and RNAi plants. Among them, plant height and effective tillers of each line were determined on eight plants, with plant height measured from the soil surface to the highest panicle top.

4.11. Statistical Analysis

The original data were compiled using MS Excel 2019. All primers were designed using Primer Premier 5 software. All data were analyzed using GraphPad Prism 8.0 for one-way ANOVA and Dunnett's multiple comparison test (*$p < 0.05$, **$p < 0.01$, ***$p < 0.001$).

Supplementary Materials: Figure S1. BLAST search with the flanking sequence of T-DNA. Figure S2. Analysis of the subcellular localization of the OsAL13 protein in rice protoplasts. Figure S3. Protein sequence encoded by *OsAL13*. Figure S4. OsAL13 protein conserved domain query in NCBI. Figure S5. *OsAL13* homologous gene search. Table S1. Cis-acting element prediction of *OsAL13* promoter region. Table S2. Subcellular localization prediction of *OsAL13* in ChloroP.

Author Contributions: DL and LC conceived the original project and research plans and supervised the experiments; XG and CW designed the experiments and performed most of the experiments; XG, CW, and QZ analyzed the data and drafted the manuscript. CD, XZ, and WL provided technical assistance; HZ, CZ and NN participated in performing the experiments. All authors supervised and complemented the writing. All authors agree to be accountable for the content of the work.

Funding: This study was supported by grants from the Central Leading Local Science and Technology Development Project (grant nos. 202207AA110010), the Key and Major Science and Technology Projects of Yunnan (grant nos. 202202AE09002102). the Applied basic research projects in Yunnan Province (grant nos. 202101AT070201). the National Natural Science Foundation of China (grant nos. 31860108).

Institutional Review Board Statement: Not applicable.

Informed Consent Statement: Not applicable.

Data Availability Statement: Not applicable.

Acknowledgments: In this section, you can acknowledge any support given which is not covered by the author contribution or funding sections. This may include administrative and technical support, or donations in kind (e.g., materials used for experiments).

Conflicts of Interest: The authors declare no conflicts of interest.

 doi:10.20944/preprints202401.1472.v1

References

1. Kirchhoff, H. Chloroplast ultrastructure in plants. *New Phytol*.**2019**,*223*,565-574.
2. Sheng, P.K.; Tan, J.J.; Jin, M.; Wu, F.Q.; Zhou, K.N.; Ma, W.W.; Heng, Y.Q.; Wang, J.L.; Guo, X.P.; Zhang, X.; et al. Albino midrib 1, encoding a putative potassium efflux antiporter, affects chloroplast development and drought tolerance in rice. *Plant Cell Rep*.**2014**,*33*,1581-1594.
3. Zhang, Y.; Tian, L.; Lu, C.M.; Chloroplast gene expression: Recent advances and perspectives. *Plant Commun*.**2023**,*4*,1-19.
4. Kusumi, K.; Iba, K. Establishment of the chloroplast genetic system in rice during early leaf development and at low temperatures. *Front. Plant Sci*.**2014**,*5*,386.
5. Gothandam, K.M.; Kim, E.S.;Cho, H.; Chung, Y.Y. OsPPR1, a pentatricopeptide repeat protein of rice is essential for the chloroplast biogenesis. *Plant Mol. Biol*. **2005**,*58*, 421-433.
6. Lin, D.; Jiang, Q.; Zheng, K.; Chen, S.; Zhou H.; Gong X.; Xu J.; Teng S.; Dong, Y. Mutation of the rice ASL2 gene encoding plastid ribosomal protein L21 causes chloroplast developmental defects and seedling death. *Plant Biol*. **2014**,*17*,599-607.
7. Zhu, X.B.; Liang, S.H.; Yin, J.J.; Yuan, C.; Wang, J.; Li W.T.; He, M.; Wang, J.C.; Chen, W.L.; Ma, B.T.; et al. The DnaJ OsDjA7/8 is essential for chloroplast development in rice Oryza sativa. *Gene*. **2015**,*574*,11-19.
8. Zhang, Z.M, Tan, J.J, Shi, Z.Y, Xie, Q.J.; Xing, Y.; Liu, C.H.; Chen, Q.L.; Zhu, H.T.; Wang, J.; Zhang, J.L.et al. Albino Leaf 1 That Encodes the Sole Octotricopeptide Repeat Protein Is Responsible for Chloroplast Development. *Plant Physiol*.**2016**,*171*, 1182-1191.
9. Wang, Y.F.; Zhang, J.H.; Shi, X.L.; Peng, Y.; Li, P.; Lin, D.Z.; Dong, Y.J.; Teng, S. Temperature-sensitive albino gene TCD5, encoding a monooxygenase, affects chloroplast development at low temperatures. *J. Exp. Bot*. **2016**,*67*,5187-5202.
10. Tang, J.P.; Zhang, W.W.; Wen, K.; Chen, G.M.; Sun, J.; Tian, Y.L.; Tang, W.J.; Yu, J.; An, H.Z.; Wu, T.T.et al. OsPPR6, a pentatricopeptide repeat protein involved in editing and splicing chloroplast RNA, is required for chloroplast biogenesis in rice. *Plant Mol. Biol*. **2017**,*95*,345-357.
11. Shen, L.; Zhang, Q.; Wang, Z.W.; Wen, H.L.; Hu, G.L.; Ren, D.Y.; Hu, J.; Zhu, L.; Gao Z.Y.; Zhang, G.H. et al. OsCAF2 contains two CRM domains and is necessary for chloroplast development in rice. *BMC Plant Biol*. **2020**,*20*,381.
12. Liu, X.; Cao, P.H.; Huang, Q.Q.; Yang, Y.R.; Tao, D.D. Disruption of a Rice Chloroplast-Targeted Gene OsHMBPP Causes a Seedling-Lethal Albino Phenotype. *Rice (N Y)*. **2020** ,*13*,1-11.
13. Chen, C.Z.; Wang, Y.L.; He, M.X.; Li, Z.W.; Shen, L.; Li, Q.; Ren, D.Y.; Hu, J.; Zhu, L.; Zhang, G.H. OsPPR9 encodes a DYW-type PPR protein that affects editing efficiency of multiple RNA editing sites and is essential for chloroplast development. *J Integr Agric*.**2023**,*22*,972-980.
14. Xu, Y.B.; Wu, Z.S.; Shen, W.; Zhou, H.Y.; Hu, L.; He, X.H.; Li, R.B.; Qin, B.X. Disruption of the rice ALS1 localized in chloroplast causes seedling-lethal albino phenotype. *Plant Sci*.**2023**,*338*,111925.
15. Yu, Q.B.; Huang, C.; Yang, Z.N. Nuclear-encoded factors associated with the chloroplast transcription machinery of higher plants. *Front. Plant Sci*.**2014**,*5*,316.
16. Castandet, B.; Germain, A.; Hotto, A.M.; Stern, D.B. Systematic sequencing of chloroplast transcript termini from Arabidopsis thaliana reveals >200 transcription initiation sites and the extensive imprints of RNA-binding proteins and secondary structures. *Nucleic Acids Res*.**2019**,*47*,11889-11905.
17. Hayashi-Tsugane, M.; Takahara, H.; Ahmed, N.; Himi, E.; Takagi, K.; Iida, S.; Tsugane K.; Maekawa, M. A mutable albino allele in rice reveals that formation of thylakoid membranes requires the SNOW-WHITE LEAF1 gene. *Plant Cell Physiol*. **2014**,*55*,3-15.
18. Zeng, X.; Tang, R.; Guo, H.; Ke, S.; Teng, B.; Hung, Y.H.; Xu, Z.; Xie, X.M.; Hsieh, T.F.; Zhang, X.Q. A naturally occurring conditional albino mutant in rice caused by defects in the plastid-localized OsABCI8 transporter. *Plant Mol. Biol*.**2017**,*94*,137-148.
19. Zhang, T.; Feng, P.; Li, Y.F.; Yu, P.; Yu, G.L.; Sang, X.C.; Ling, Y.H.; Zeng, X.Q.; Li, Y.D.; Huang, J.Y. et al. VIRESCENT-ALBINO LEAF 1 regulates leaf color development and cell division in rice. *J. Exp. Bot*.**2018**,*69*,4791-4804.
20. Li, W.R.; Zhang, Y.C.; Anisur Rahman Mazumder, Md.; Pan, R.H.; Akhter, Delara. Research progresses on rice leaf color mutants. *Crop Design*.**2022**,*1*,1-5.
21. Yoo, S.C.; Cho, S.H.; Sugimoto, H.; Li J.; Kusumi, K.; Koh, H.J.; Iba, K.; Paek, N.C. Rice virescent3 and stripe1 encoding the large and small subunits of ribonucleotide reductase are required for chloroplast biogenesis during early leaf development. *Plant Physiol*.**2009**,*150*, 388-401.
22. Li, X.; He, Y.; Yang, J.; Jia, Y.H.; Zeng, H.L. Gene mapping and transcriptome profiling of a practical photo-thermo-sensitive rice male sterile line with seedling-specific green-revertible albino leaf. *Plant Sci*.**2018**,*266*,37-45.
23. Lee, S.; Masclaux-Daubresse, C. Current understanding of leaf senescence in rice. *Int. J. Mol. Sci*.**2019**,*22*,1-19.

24. Garton, S.; Knight, H.; Warren, G.J.; Knight, M.R.; Thorlby, G.J. crinkled leaves 8-A mutation in the large subunit of ribonucleotide reductase-leads to defects in leaf development and chloroplast division in Arabidopsis thaliana. *Plant J*. **2007**, *50*,118-127.
25. Jiang, Q.; Ma, X.; Gong, X.; Zhang, J.; Teng, S.; Xu, J.; Lin, D.; Dong, Y. The rice OsDG2 encoding a glycine-rich protein is involved in the regulation of chloroplast development during early seedling stage. *Plant cell rep*.**2014**,*33*, 733-744.
26. Jiang, Q.; Mei, J.; Gong, X.D.; Xu, J.L.; Zhang, J.H.; Teng, S.; Lin, D.Z.; Dong, Y.J. Importance of the rice TCD9 encoding α subunit of chaperonin protein 60 (Cpn60α) for the chloroplast development during the early leaf stage. *Plant Sci*.**2014**,*215-216*,172-179.
27. Zeng, X.; Tang, R.; Guo, H.; Ke, S.; Teng, B.; Hung, Y.H.; Xu, Z.; Xie, X.M.; Hsieh, T.F.; Zhang, X.Q. A naturally occurring conditional albino mutant in rice caused by defects in the plastid-localized OsABCI8 transporter. *Plant Mol Biol*.**2017**,*94*,137-148.
28. Zhou, K.; Zhang, C.; Xia, J.; Yun, P.; Wang, Y.; Ma, T.; Li, Z. Albino seedling lethality 4; Chloroplast 30S Ribosomal Protein S1 is Required for Chloroplast Ribosome Biogenesis and Early Chloroplast Development in Rice. *Rice (N Y)*.**2021**,*14*, 47.
29. Zheng, H.; Wang, Z.R.; Tian, Y.L.; Liu, L.L.; Lv, F.; Kong, W.Y.; Bai, W.T.; Wang, P.R.; Wang, C. L.; Yu, X.W.et al. Rice albino 1, encoding a glycyl-tRNA synthetase, is involved in chloroplast development and establishment of the plastidic ribosome system in rice. *Plant Physiol. Biochem*.**2019**,139,495-503.
30. Wu, Q.; Zhang, C.; Chen, Y.; Zhou, K.; Zhan, Y.; Jiang, D. OsCpn60β1 is Essential for Chloroplast Development in Rice Oryza sativa L. *Int. J. Mol. Sci*.2020,21,4023.
31. Emanuelsson, O.; Nielse, H.; Heijne, G, V. ChloroP, a neural network-based method for predicting chloroplast transit peptides and their cleavage sites. *Protein Sci*. **1999**, 8,978-984.
32. Adam, Z.; Charuvi, D.; Tsabari, O.; Knopf, R.R.; Reich, Z. Biogenesis of thylakoid networks in angiosperms: knowns and unknowns. *Plant Mol. Biol*.**2011**,76, 221-234.
33. Leister, D. Chloroplast research in the genomic age. *Trends Genet*.**2003**,19,47-56.
34. Rodriguez-Villalon, A.; Gas, E.; Rodriguez-Concepcion, M. Phytoene synthase activity controls the biosynthesis of carotenoids and the supply of their metabolic precursors in dark-grown Arabidopsis seedlings. *Plant J*.**2009**, *60*,424-435.
35. Meier, S.; Tzfadia, O.; Vallabhaneni, R.; Gehring, C.; Wurtzel, E.T. A transcriptional analysis of carotenoid, chlorophyll and plastidial isoprenoid biosynthesis genes during development and osmotic stress responses in Arabidopsis thaliana. *BMC Syst. Biol*.**2011**,*5*,1-19.
36. Hussain, A.; Peng, J. DELLA Proteins and GA Signalling in Arabidopsis. *J. Plant Growth Regul* .**2003**,*22*,134-140.
37. Kobayashi, K.; Ohnishi, A.; Sasaki, D.; FujiiS.; Iwase A.; Sugimoto, K.; Masuda, T.; Wada, H. Shoot Removal Induces Chloroplast Development in Roots via Cytokinin Signaling. *Plant Physiol*.**2017**,*173*,2340-2355.
38. Sauter, M. Differential expression of a CAK (cdc2-activating kinase)-like protein kinase, cyclins and cdc2 genes from rice during the cell cycle and in response to gibberellin. *Plant J* .**1997**,*11*,181-90.
39. Toki, S.; Hara, N.; Ono, K.; Onodera, H.; Tagiri, A.; Seibi, Oka.; Hiroshi, Tanaka. Early infection of scutellum tissue with Agrobacterium allows high-speed transformation of rice. Plant J. **2006**,47,969-976.
40. Arocho, A.; Chen, B.Y.; Ladanyi, M.; Pan, Q.L. Validation of the $2^{-\Delta\Delta Ct}$ calculation as an alternate method of data analysis for
41. quantitative PCR of BCR-ABL P210 transcripts. *Diagn. Mol. Pathol*. **2006**, *15*, 56–61.
42. Poddar, S.; Tanaka, J.; Cate, J.H.D.; Staskawicz, B.; Cho M.J. Efficient isolation of protoplasts from rice calli with pause points and its application in transient gene expression and genome editing assays. *Plant Methods*.**2020**,16:151.
43. Zhu, Q.; Zhang, X.L.; Nadir, S.; DongChen, W.H.; Guo, X.Q.; Zhang, H.X.; Li, C.Y.; Chen, L.J.; Lee, D.S. A LysM Domain-Containing Gene OsEMSA1 Involved in Embryo sac Development in Rice (Oryza sativa L.). *Front. Plant Sci*.**2017**,*8*,1-13.